

Topological singularities and transport in kicked Harper model

Indubala I. Satija

Department of Physics, George Mason University, Fairfax, Virginia 22030, USA

(Received 7 June 2004; revised manuscript received 19 January 2005; published 27 May 2005)

Quasienergy spectrum of kicked Harper model is found to exhibit a series of diabolic crossings. These conical degeneracies reside mostly on the symmetry line of its two-dimensional parameter space and their locations are found to coincide with the local maxima of the kinetic energy of the kicked system. Additionally, there are exceptional point singularities, that are found by analytically continuing the kicking parameter in the complex plane. The location of these singularities appear to be correlated with the localization of the quantum wave packet. These studies suggest a correlation between the transport and the topological characteristics of the system.

DOI: 10.1103/PhysRevE.71.056213

PACS number(s): 05.45.Mt, 03.65.Vf

I. INTRODUCTION

Double-cone or diablo geometry characterizes the accidental spectral degeneracies of a typical quantum systems with a real Hamiltonian. Such degenerate points are referred as Diabolic points [1] (DP) and correspond to the special points where the eigenfunctions are not single-valued: as one varies parameters in a closed loop enclosing the point, the wave functions acquire a phase factor, known as Berry phase, that depends on the history of the path and hence is of purely geometric origin. It is interesting that the occurrence of this crossing of eigenvalues in parameter space is sensed by a circuit that does not pass through the degeneracy, but simply encloses it. This is analogous to the electrostatics where the Gauss sphere of arbitrary radius detects an electric charge. In fact, the presence of a DP leads to monopole-type singularity with a fictitious (geometric) monopole at the diabolic point [2]. The importance of DPs has been emphasized in molecular as well as in nuclear spectra [2].

Another type of singularity that has been the subject of many recent studies is known as exceptional point (EP) [3]. At an EP, two eigenvalues coalesce and the corresponding eigenvectors become parallel and hence the eigenspace of the two coalescing levels becomes one-dimensional. As illustrated by Kato [3] in his book, EPs can occur in real as well as in complex plane and may correspond to a branch point of an analytic function. However, as emphasized by Kato, an EP need not be a branch point. For 2-level systems, EPs have been found in the vicinity of level repulsion, when analytic continuation in the complex space connects the two levels by a branch point [4]. The significance of EPs has been discussed in dissipative resonators and the experiments have confirmed the topology underlying an EP [5]. Furthermore, the influence of these points on transmission through quantum dots was discussed recently [6]. The DPs and the EPs are topological singularities that are the subject of this paper. Here, we illustrate the importance of these topological singularities in the transport characteristics of a nonintegrable system whose classical limit exhibits chaotic dynamics.

As pointed out by Berry [7], when detached from their original quantum mechanical context, the diabolic connection and the associated geometric phase is in fact a property of matrices. In the simplest case of real symmetric 2×2

matrices, the eigenvectors change sign as one changes two parameters around a closed circuit which encloses a diabolic degeneracy. Essential aspects of DPs as well as EPs have been discussed using 2×2 matrices [1,4]. As we discuss below, the spectral characteristics of the kicked Harper model [8,9] with Planck constant $\hbar/2\pi=1/N$ (N is an integer), exhibit a series of topological singularities whose exploration involves the study of $N \times N$ matrices. The special case of $N=2$ corresponds to one of the most dominant resonance of the model. Here we study the spectral characteristics of $N=2$ case analytically while the higher N cases are analyzed numerically. Our studies complement earlier discussion of the DPs and the EPs as the matrices under investigation are unitary for real parameters and complex without being symmetric for complex parameter values. Additionally, we also discuss the band spectrum of the model and demonstrate a relationship between the topology and transport in the system. Furthermore, we briefly discuss $N>2$ cases. However, detailed analysis of the singularities in these cases is very complicated.

This paper is organized as follows. In Sec. II, we briefly discuss the kicked Harper model. In Sec. III, we provide detailed spectral analysis of the $N=2$ resonance and discuss the topological singularities of the spectrum in real and in complex parameter space. The band spectrum and the transport properties and their relationship with the topological singularities are discussed in Sec. IV. Section V describes the $N=6$ resonance and briefly discusses higher N cases. In Sec. VI, we summarize our conclusions and discuss various open issues.

II. KICKED HARPER MODEL

Periodically kicked Harper Hamiltonian characterized by two parameters L and K is

$$H(t) = L \cos(p) + K \cos(q) \sum_{k=-\infty}^{\infty} \delta(t-k). \quad (1)$$

Here p and q are respectively the momentum and the position operators. For the δ -kicked system, the time evolution operator U for one period, with $U\psi(t)=\psi(t+1)$ factors as

$$U = \exp[-iL \cos(p)/\hbar] \exp[-iK \cos(q)/\hbar]. \quad (2)$$

Here, \hbar is typically an effective Planck's constant. The first term governs the free evolution between the kicks while the second term describes the effect of kicking.

The model has been studied in various contexts in classical as well as in the quantum limits [9]. In its two-dimensional parameter space, the quantum dynamics of this non-integrable mixed phase space system is extremely complex. For incommensurate case, where $\hbar/2\pi$ is an irrational number, the model exhibits localized as well as ballistic transport for $K \neq L$. In this case, intricately nested localized and ballistic phases for $L > K$ have their dual image of ballistic and localized phases for $K > L$ [10]. This is a consequence of self-duality along the symmetry line, $K=L$ along which the eigenfunctions and the spectrum exhibit fractal characteristics.

For the case where $\hbar/2\pi$ is a rational number, the model exhibits quantum resonances and the quasienergy states are extended for almost all values of K and L and the quantum transport is ballistic. In this resonant regime, the significance of self-duality is not clear. In this paper, we will only consider this case and write $\hbar/2\pi = 1/N$, where N is a positive integer. Since the time evolution operator U is periodic in p , it can be reduced to a $N \times N$ matrix that depends upon the Bloch vector κ [11]. Varying κ is like varying boundary conditions, and summing over all boundary conditions give us a band of states, and a band of eigenvalues. Special case of $\kappa=0$, corresponds to periodic boundary conditions. As N increases, the widths of the quasienergy bands decrease and therefore higher order resonances are difficult to observe in an experiment. In fact $N=1, 2$ were the subject of very extensive theoretical and experimental studies in a kicked rotor model [12,13].

Due to the periodicity of Hamiltonian in t , we consider the floquet states, $\psi(t) = e^{i\omega t} \phi_\omega(t)$. Here ω is the quasienergy of the system and $\phi_\omega(t) = \phi_\omega(t+1)$. This leads to an eigenvalue equation for $U: U\phi_\omega = e^{i\omega} \phi_\omega$. Its matrix elements are computed in the plane wave basis e^{imq} where $\hbar m$ is the quantized angular momentum of the unkicked system. We have N eigenstates, parametrized by the Bloch vector κ . In this paper, we explore the model analytically for $N=2$ and study higher order resonances numerically. For investigating topological singularities, we study the model for real kicking parameter K as well as for the case where K is analytically continued in the complex plane.

III. SPECTRAL ANALYSIS FOR $N=2$ RESONANCE

For $N=2$, the one-step time evolution operator in the plane wave basis is a 2×2 matrix,

$$\begin{pmatrix} e^{-i\bar{L}} \cos(\zeta \bar{K}) & -ie^{-i(\bar{L}+\kappa)} \sin(\zeta \bar{K}) \\ -ie^{i(\bar{L}+\kappa)} \sin(\zeta \bar{K}) & e^{i\bar{L}} \cos(\zeta \bar{K}) \end{pmatrix},$$

where $\bar{K} = K/\hbar$ and $\bar{L} = L/\hbar$ and $\zeta = \cos(\kappa)$. For real K and L , this matrix is unitary.

The eigenvectors of the matrix can be written as

$$e_1 = [\cos(\beta) e^{i\phi}, \sin(\beta) e^{-i\phi}], \quad (3)$$

$$e_2 = [\sin(\beta) e^{-i\phi}, -\cos(\beta) e^{i\phi}]. \quad (4)$$

Here β and ϕ are given by

$$\tan(\beta) = [\sin(\bar{L}) \cos(\zeta \bar{K})] + \frac{\sqrt{[1 - \cos^2(\zeta \bar{K}) \cos^2(\bar{L})]}}{\sin(\zeta \bar{K})}, \quad (5)$$

$$\phi = -(\pi/2 + \bar{L}/2).$$

The corresponding eigenvalues are

$$e^{i\omega_{1,2}} = \cos(\bar{L}) \cos(\zeta \bar{K}) \pm i \sqrt{[1 - \cos^2(\bar{L}) \cos^2(\zeta \bar{K})]}. \quad (6)$$

As seen from Eq. (6), the eigenvalues become degenerate when the quantity in the square root vanishes. This happens when $\bar{L} = n\pi$ and $\zeta \bar{K} = m\pi$. Additionally, there is another degeneracy when $\cos(\bar{L}) \cos(\zeta \bar{K}) = \pm 1$ that occurs for complex parameters. In this case, the two eigenvalues are branches of one double-valued analytic function that meet at the branch point. As we discuss below, these degeneracies are topological singularities that are relevant in the transport properties of the system.

We analyze the degeneracies of the 2-level (fixed κ) and 2-band (with $0 \leq \kappa \leq \pi$) system. In addition to analytic analysis of these singularities, they are also shown graphically in the figures. This graphical representation of $N=2$ spectrum facilitates detailed comparison with $N > 2$ resonances and this in turn provides better understanding of higher N resonances for which theoretical analysis is not possible. Figures 1–3 show quasienergy spectrum for real as well as for complex kicking parameter K , with main focus being to illustrate the interesting topological structures associated with the spectral characteristics of the model.

We first discuss the $\kappa=0$ ($\zeta=1$) case. For real K and L , the two levels are degenerate with $\omega_c = 0 \pmod{2\pi}$, at the critical values of the parameter, $\bar{K}_c = n\pi$, $\bar{L}_c = m\pi$. The crossings for $\kappa=0$ at K_c and L_c are diabolic in K - L space. This can be seen in two ways. First, since $\cos(\omega) = \cos(\bar{K}) \cos(\bar{L})$ [from Eq. (6)], linearizing about the critical points $\bar{K}_c = \bar{L}_c$, we get $(\bar{K} - \bar{K}_c)^2 + (\bar{L} - \bar{L}_c)^2 = (\omega - \omega_c)^2$, which is the equation of a cone. This implies conical intersection in ω - K - L plane (see Fig. 2). Secondly, the diabolic character of this point can also be seen by considering a small parametric loop of radius r around this point: $K = K_c + r \cos \theta$ and $L = L_c - r \sin \theta$ as we vary $0 \leq \theta \leq 2\pi$. Linearizing in r , from Eq. (5) we get $\tan \beta \approx -\tan(\pi/4 - \theta/2)$. Thus as we go around the crossing points $K_c = L_c = n\pi^2$, $\theta \rightarrow \theta + 2\pi$, and $\beta \rightarrow \beta + \pi$ and hence the wave functions change sign.

We next discuss the crossings in the complex plane. As seen from Eq. (6), for $\kappa=0$, this occurs when $\cos(\bar{K}) = 1/\cos(\bar{L})$. With L real, and K imaginary ($K \rightarrow iK$), the quasienergies along the imaginary K axes with $|K|=L$ are given by

$$e^{i\omega_{1,2}} = \cos(\bar{K}) \cosh(\bar{K}) \pm i \sqrt{[1 - \cos^2(\bar{K}) \cosh^2(\bar{K})]}. \quad (7)$$

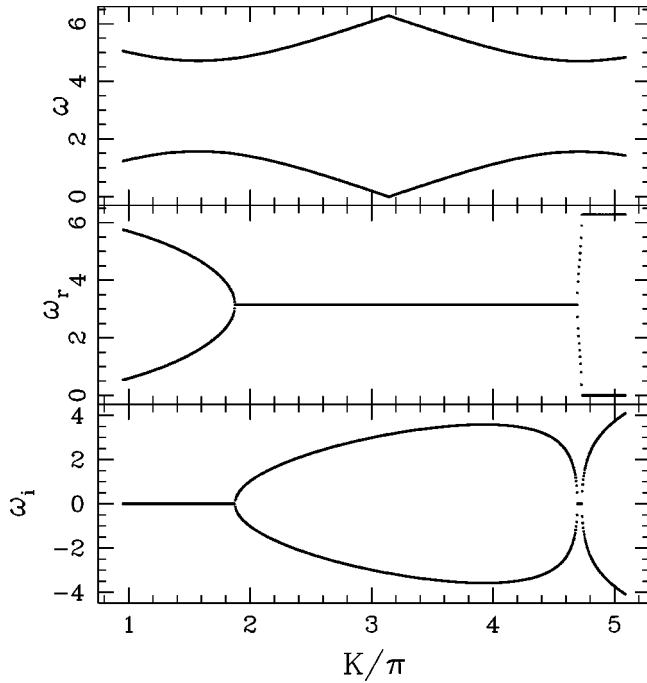


FIG. 1. For $N=2$, figure shows the quasienergy spectrum for periodic boundary conditions ($\kappa=0$). The top figure corresponds to real parameters on the symmetry line ($K=L$). The middle and the lowest figures, respectively, show the real and the imaginary part of the spectrum for imaginary $K(K_r=0)$ with $|K|=L$. This choice is dictated by the fact that EPs reside along this line in complex K plane. The constancy of ω_r as well as ω_i as seen in some parts of the parametric windows is due to $K_r=0$ as in the complex K plane; we typically see two distinct ω_r and ω_i as clarified in Fig. 3.

In the complex K plane, there is a degeneracy when $\cosh(\bar{K})=1/\cos(\bar{L})$. For large K ($\bar{K}>1$), this happens in close proximity to $\bar{L}=(2n+1)\pi/2$. To see the relationship between the crossings in the complex K plane and the avoided crossings in the real parameter space, we note that for $\kappa=0$ on $K=L$ line, the avoided crossings correspond to the $d\omega/dK=0$. These exist mid way between the diabolic crossings: that is at $\bar{K}=\bar{L}=(2n+1)\pi/2$, with $n=1, 2, \dots$

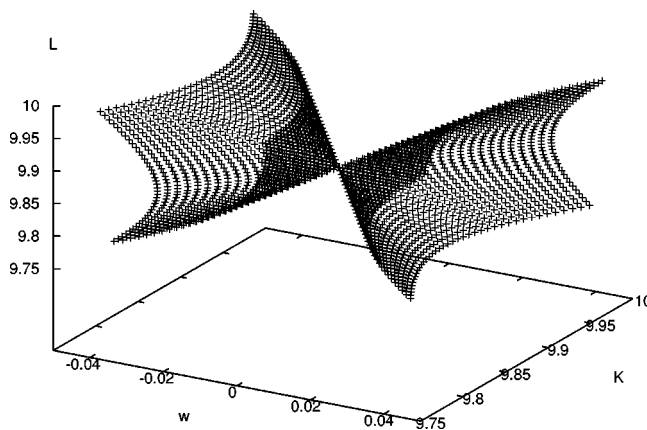


FIG. 2. Diaboloic geometry near $K=L=\pi^2$, $\omega=0$ showing ω - K - L surface for $\kappa=0$ in $N=2$ case.

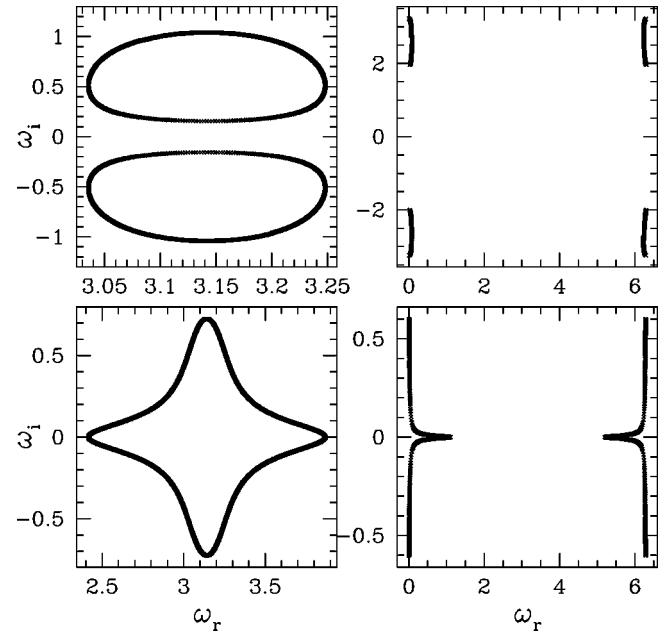


FIG. 3. Figure shows the topology associated with $N=2$ quasienergies when a closed circuit in complex K plane does not enclose an EP (top) and encloses an EP (bottom). The figures on the left and right respectively correspond to the EPs near $K=1.89\pi$ and $K=4.75\pi$. Note that since ω_r is defined mod 2π , the figures on the right correspond to two loops at the top and a single loop at the bottom.

The complex conjugate eigenvalues $\omega=\omega_r\pm i\omega_i$ coalesce when the quantity in the square root in Eq. (7) vanishes. We will denote this quantity as Δ , where $\Delta=1-\cos^2(\bar{K})\cosh^2(\bar{K})$. It should be noted that when $\Delta>0$, $\omega_i=0$ and when $\Delta<0$, $\omega_r=0, \pi$. The degenerate points in the complex K plane are branch points where $\Delta=0$, $\omega_i=0$ and $\omega_r=0$ or π . Unlike Diaboloic crossing, the eigenvectors of the two coalescing levels become parallel. Within an overall constant, such an eigenvector is given by $e=(1, ie^{-i\bar{K}})$. This implies that the branch point singularities are exceptional points due to the *exceptional* properties related to the incompleteness of the function space.

As shown in Fig. 1, with the exception of the first point, all other EPs come in pairs and we will refer them as twin EPs. This is because as K increases, Δ is negative except in the neighborhood of $K=(2n+1)\pi/2$. We write $K=(2n+1)\pi/2+\epsilon$ (where ϵ is small) and linearize Δ in ϵ . This gives $\Delta=0$ when $\epsilon\approx\pm e^{-(2n+1)\pi/2}$, resulting in twin EPs. Clearly, the parametric distance between the twin EPs goes to zero exponentially as K becomes large.

The EPs in the complex plane are located in the vicinity of the the avoided crossings when K is analytically continued in the complex K plane. As discussed earlier, for values of $\bar{K}>1$, the EPs occur exponentially close to $\bar{K}=(2n+1)\pi/2$ along the imaginary K axis, which are the locations of the avoided crossings for real K .

The exceptional points are genuine crossings in the complex K plane where both the real and the imaginary part of ω coalesce. Additionally, there are crossings associated either

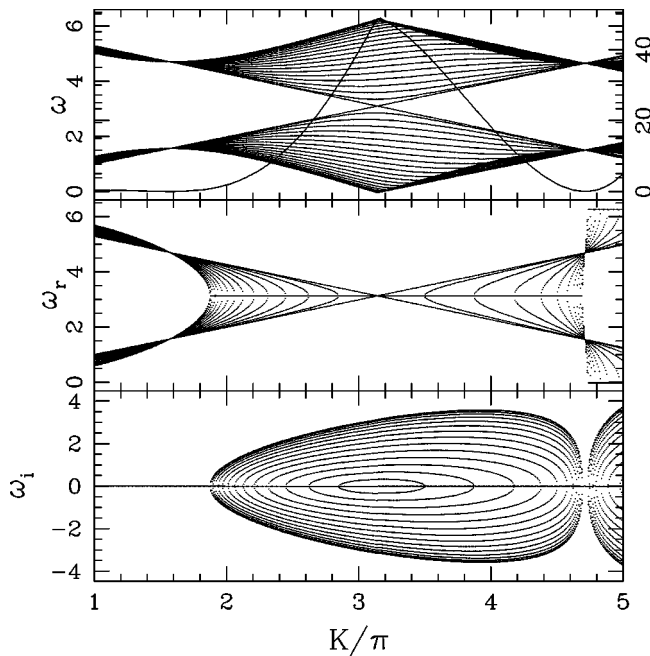


FIG. 4. Figure shows the quasienergies obtained using 30 different values of κ , covering most parts of the bands. Similar to Fig. 1, the top figure shows the band structure along the symmetry line for real K . The middle and the bottom part of the figure shows the real and the imaginary part of the energies when K is moved along the imaginary axis. In the top figure, we also show the kinetic energy along the symmetry line.

with the real or the imaginary part of the quasienergies. Such crossings have been referred as type I and type II, respectively [13]. As seen in Fig. 1, along the imaginary K axis, the location of EPs coincide with that of type I and type II crossings. To illustrate the changes in topologies due to EPs, we follow quasienergies along a closed circuit in the complex K plane, with or without enclosing the EPs (Fig. 3). If no EP is encircled, the eigenvalues trace out two disconnected loops. However, when an EP is encircled, the two circuits merge into a single circuit.

IV. BAND SPECTRUM AND TRANSPORT FOR $N=2$

We now discuss the quasienergy bands, the continuum of the energy levels, obtained by varying κ in the closed interval $(0, \pi)$ (see Fig. 4). In addition to the quasienergy bands for the real parameters along the symmetry line, we also show the complex bands when K is moved along the imaginary axis. As discussed below, the DPs, the EPs as well as the type I and type II crossings emerge with special significance when viewed in the context of the band structure.

First, the location of diabolic crossings at $K_c=L_c$ corresponds to the points where the two bands merge. These crossings for $\kappa=0$ become a family of avoided crossings as the Bloch vector κ becomes nonvanishing. [Only exception being the $\kappa=\pi/2$ ($\zeta=0$) case, where the levels cross but this crossing is not diabolic in K - L space.] As K is moved along the imaginary axis, the diabolic crossing transforms into an accumulation point of type II crossing. At this point, the real

part of the quasienergy band collapses. In other words, the band at diabolic crossings move to the imaginary axis when K becomes imaginary.

Secondly, in the vicinity of EPs, there is a *band collapse* and hence an infinite-fold degeneracy for real as well as for imaginary K . For the real part of the spectrum, we have two different accumulation points of type II crossings corresponding to two bands. For the imaginary part of the spectrum, there is one accumulation point of type I crossing where different levels, characterized by different κ meet. As we will discuss later, all the above characteristics of the quasienergy bands persist for higher N cases.

To investigate the importance of topological singularities, we numerically calculate the kinetic energy of the model, (using plane wave initial conditions) for fixed number of kicks. The quantum transport is found to be ballistic except at parameter values where there is a band collapse. At these isolated parameter values, the quantum wavepacket is found to remain localized, that is, the momentum does not increase with time. In view of the fact that for rational \hbar , the quantum transport is ballistic for almost all values of the parameters K and L , we write the kinetic energy of the system as $\langle p^2/2 \rangle = At^2$. For a fixed time t , as K varies, the changes in the kinetic energy are due to changes in the parameter A .

As we vary the parameter K , the kinetic energy shows oscillatory behavior with peaks and valleys that appear to be correlated with the topological singularities. At diabolic crossings, the kinetic energy exhibits a local maximum. However, it should be noted that all local maxima in the kinetic energy are not associated with the diabolic crossing. Interestingly, as seen in Fig. 5, the kinetic energy exhibits nonanalytic dependence on K at the diabolic points. The peak at $\bar{K}=1$ where A varies smoothly with K is not associated with a diabolic crossing. However, peaks at $K/\pi=\pi$ and $K/\pi=2\pi$, where dA/dK is nonanalytic, are in fact correlated with the diabolic points.

In the vicinity of the EPs, the quantum transport is localized in both x and p . In other words, the momentum of the system does not increase as the system is kicked. In contrast, the presence of a DP does not affect the ballistic aspect of the transport, but it leads to a nonanalytic dependence of kinetic energy on the kicking parameter.

V. SPECTRAL AND TRANSPORT ANALYSIS FOR $N=6$

As N increases, detailed analysis of the singularities become very complicated. Our numerical analysis suggests that various crossing scenarios and the associated EPs and DPs as discussed above may continue to exist for $N>2$. Figures 6–9 illustrate this for $N=6$ resonance. The diabolic aspect of the crossing at $K \approx 1.4\pi$ for $\kappa=0$ is shown in Fig. 7. New aspect here is that the conical intersection of two energy surfaces is intercepted at the diabolic point, by an another energy surface. This topological singularity leaves its fingerprints in the complex K plane. With K along the imaginary axis, we see a pair of crossings symmetrically placed about $\omega_i=0$ as seen in Fig. 6 (bottom) and further in the complex plane in Fig. 8. In addition, there are crossings at $K \approx 1.65\pi i$ and at $K \approx 1.85\pi i$, where we also have type I and type II crossings.

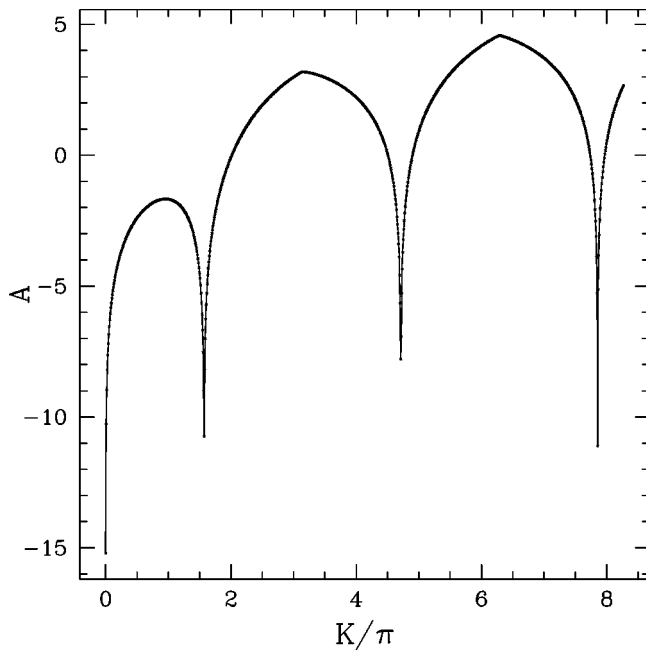


FIG. 5. Variation in the constant A (on the log scale), as K is varied along the symmetry line. The solid line and the dots respectively correspond to $t=400$ and $t=800$ kicks. The fact that the two data sets coincide confirms the fact that the transport remains ballistic at almost all values of K . The first peak at $K/\pi=1$ corresponds to the point where the bandwidth exhibits a local maxima. However, at this point, the bands do not cross and there is no diabolic point. The characteristic “dips” in the figure correspond to localized transport and occur in the vicinity of the EPs.

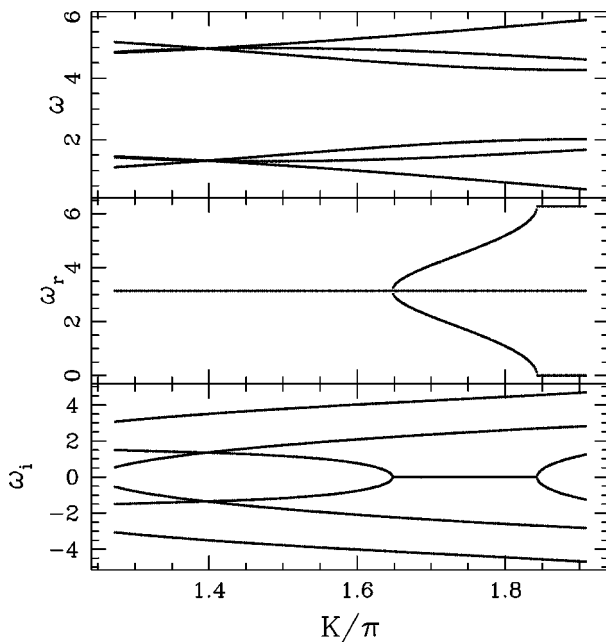


FIG. 6. Same as Fig. 1 with $N=6$. Near $K \approx 1.4\pi$, we have a pair of diabolic crossings for $\kappa=0$, as well as a pair of crossings in the complex K plane. Additionally, there are EPs at $K \approx 1.65\pi$ and $K \approx 1.85\pi$.

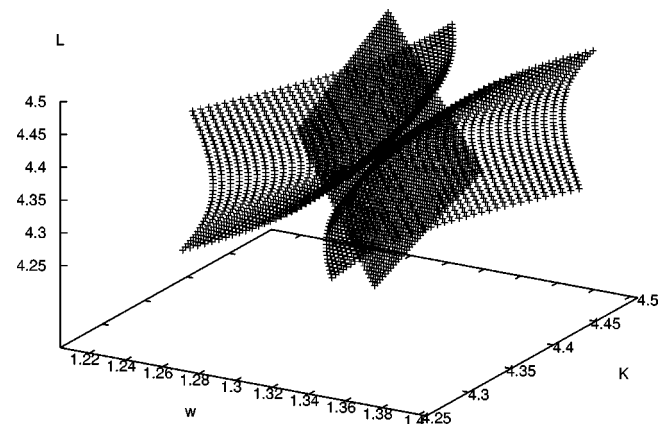


FIG. 7. The figure shows three of the ω - K - L surfaces for $\kappa=0$ in $N=6$ resonance. Two of the surfaces show conical intersection at $K=L \approx 1.4\pi$ while the third surface simply passes through the DP.

Changes in the topologies as we encircle such crossings are shown in Fig. 8. The figure clearly illustrates the differences in the crossings at $K/\pi \approx 1.4$ and at $K/\pi \approx 6.5$.

Figure 9 illustrates variations in the quasienergy bands as well as in the kinetic energy for $N=6$ case as K is varied. In analogy to $N=2$ case, the location of the diabolic crossing coincides with the location of band merging which in turn coincides with the location of maximum of the kinetic energy. For K along the imaginary axis, the real part of the corresponding quasienergy bands collapse as was the case for $N=2$ resonance. Finally, analogous to $N=2$ case, the local minimum of the kinetic energy is located in the vicinity of the band collapse.

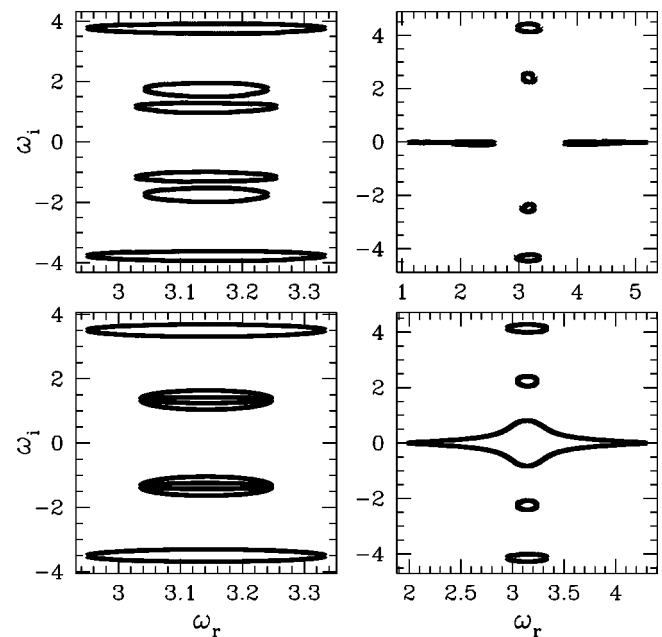


FIG. 8. The figure shows quasienergies for the $N=6$ case, when the parameters are varied in closed loops centered at $K_i=L=1.4\pi$ (left) and $K_i=L=1.6\pi$ (right). The top figures correspond to the cases when the closed circuits do not enclose the crossings while the bottom figure corresponds to the loops that enclose the crossings.

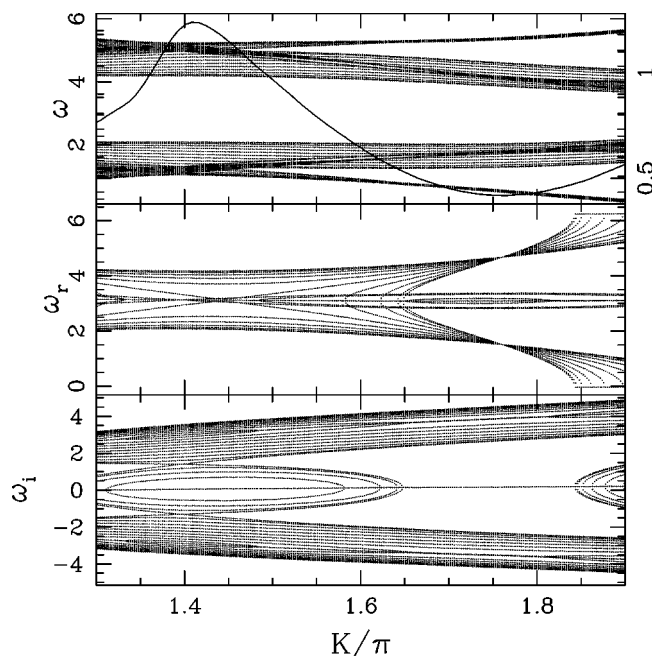


FIG. 9. Same as Fig. 4 for the $N=6$ case showing six quasienergy bands and the kinetic energy.

As N increases (or \hbar decreases), analysis of topological singularities become difficult. Detailed study of topological singularities in the semiclassical limit is beyond the scope of this paper. However, we believe that the locations of DPs in parameter space may be correlated with the location of the accelerator modes [14] in the corresponding classical system as $\hbar \rightarrow 0$. This is due to the fact that in the semiclassical limit, the enhancements in the quantum transport can be usually traced to the enhancements in the classical transport which have their origin in the accelerator modes. An example of this is shown in Fig. 10 where we compare the classical and the quantum kinetic energy as N increases. We would like to emphasize that the quantum transport is mostly ballistic (due to rationality of $\hbar/2\pi$), whereas the corresponding classical transport depends strongly on parameters and varies from subdiffusive, diffusive to superdiffusive. For a fixed finite time, the variation in quantum transport is described in terms of the parameter A while the appropriate quantity for classical transport is the exponent β , defined as $\langle p^2 \rangle \approx t^\beta$ where $0 \leq \beta \leq 2$. Narrow peaks in the classical transport, due to accelerator modes have their fingerprints in broad quantum peaks. The shift in the quantum peaks relative to the corresponding classical peaks is due to large \hbar . As the Planck constant increases, the quantum system fails to resolve the tiny accelerator islands associated with the classical system, however, the transients (finite t dynamics) appear to sense some signature of anomalous classical transport that result in broad peaks.

Detailed study of various resonances in two-dimensional K - L parameter space shows that the diabolic crossings are mostly confined to the $K=L$ line. In our numerical exploration, all crossings with $\kappa=0$ on the symmetry line were found to be diabolic, irrespective of the N values. We would also like to mention that diabolic crossings were also seen

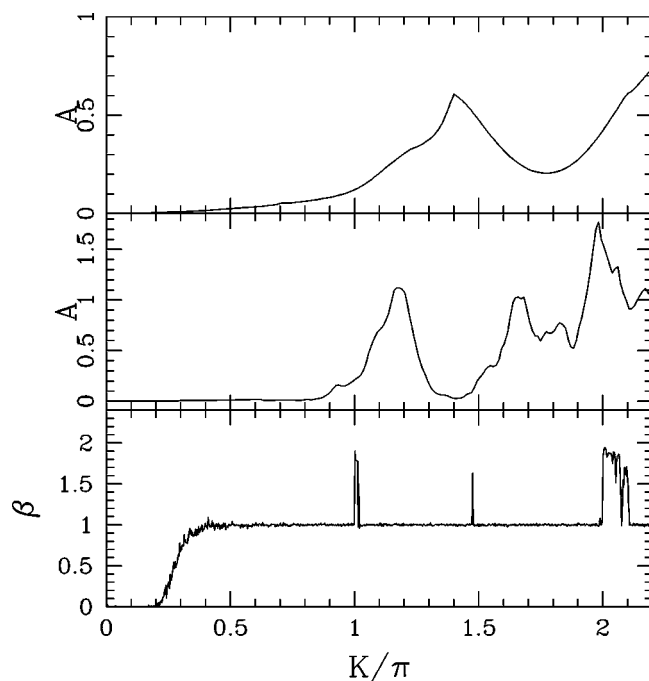


FIG. 10. Figure shows the variation in kinetic energy as the parameter K varies along the symmetry line. The upper and the middle curve respectively corresponds to $N=6$ and $N=20$. The bottom figure shows the classical exponent, where $\beta > 1$ indicates superdiffusion. The origin of spikes at $K/\pi=1$ and $K/\pi \approx 1.48$ is due to period-2 accelerator modes while that at $K/\pi=2$ corresponds to period-1 accelerator mode.

for other values of κ . For example, for $N=10$, there exists a DP at $\omega=0$, with $K=L \approx \pi$ when $\kappa \approx 0.275\pi$. We have discussed crossings only on the symmetry line, $K=L$ (or $|K|=L$, for imaginary K). As we move away from the symmetry line, $K \neq L$, diabolic crossings for $N=2$ case were found only at $\bar{K}=n\pi$ and $\bar{L}=m\pi$. However, avoided crossings continue to exist throughout the two-dimensional parameter space.

VI. SUMMARY AND CONCLUSIONS

In summary, the kicked Harper model provides an interesting example of a nonintegrable system exhibiting topological singularities. The study of topological singularities in $N=2$ resonance is somewhat analogous to earlier studies of these singularities using 2×2 matrices. The aspect here is the different perspective that emerges when topological singularities are viewed in the context of band structure and the transport properties of the system. Importance of the diabolic as well as the exceptional point singularities lies in the fact that their locations appear to be correlated with the extrema of the kinetic energy.

The EPs are found in the vicinity of the localized transport of the system while the DPs occur at parameter values where the kinetic energy exhibits local maximum, with a characteristic nonanalytic behavior. Diabolic crossings when continued in the complex plane, are found to be associated with an accumulation point of type II crossings. Our study unveils many interesting features of the quasienergy bands

and their relation with the topology. Analytical understanding of the correlation between the band width enhancement, the diabolic crossing and the nonanalytic character of the kinetic energy remains an interesting open problem.

Importance of topology in delocalization of symmetric kicked Harper was the subject of an earlier study [8]. To what extent, topological singularities influence localization properties is therefore an important question. The generality of the relationship between the EPs and the localization that surfaced in our analysis here requires further investigation. It should be noted that on the symmetry line, the localized transport exists at isolated points. However, for $N=2$ case, it is clear from Eq. (6) that $\bar{L}=(2n+1)\pi/2$ describes a critical line in K - L parameter space where we have infinite degeneracy and if one starts in a localized state in q or p , one stays in such a state. In other words, at these points the kinetic energy does not grow with time. Fate of these critical lines (with localized transport) as N increases requires detailed study of the model in two-dimensional parameter space.

The study of quantum transport in systems whose classical limit is chaotic is one of the most active frontiers. Therefore, many key questions linking transport and topology arise in the semiclassical limit. However, in this limit, detailed analysis of the topological singularities is very complicated.

Therefore, the usefulness of this type of study in the semiclassical limit remains open.

Various experimental realizations of kicked Harper have been proposed [15]. In view of the experimental relevance of the $N=2$ resonance in kicked particle problem [12], the $N=2$ resonance of the kicked Harper model may also be of experimental interest. In fact the kicked particle or rotor in the presence of gravity may be an important 2-parameter model for investigating a relation between topology and transport. In general, finding topological singularities, by numerically detecting a crossing point can be quite demanding. However, since their location coincides with the minimum or the maximum of the kinetic energy, we have an easier method to trace the topological singularities. By correlating transport and topological singularities, one may have a new experimental realization of the fascinating conical and branch point topologies.

ACKNOWLEDGMENTS

The research of I.I.S. was supported by National Science Foundation Grant No. DMR 0072813. I would like to thank Shmuel Fishman for various comments.

-
- [1] M. V. Berry, Proc. R. Soc. London, Ser. A **392**, 45 (1984).
 - [2] For collection of various papers, see F. Wilczek and A. Shapere, *Geometric Phases in Physics* (World Scientific, Singapore, 1989).
 - [3] T. Kato, *Perturbation Theory of Linear Operators* (Springer, Berlin, 1966).
 - [4] W. D. Heiss, M. Muller, and I. Rotter, Phys. Rev. E **58**, 2894 (1998).
 - [5] O. Latinne *et al.*, Phys. Rev. Lett. **74**, 46 (1995); C. Dembowski *et al.*, *ibid.* **86**, 787 (2001); Phys. Rev. E **69**, 056216 (2004).
 - [6] I. Rotter and A. F. Sadreev, Phys. Rev. E **69**, 066201 (2004).
 - [7] Michael Berry, Phys. Today **43** (12), 34 (1990).
 - [8] P. Leboeuf, J. Kurchan, M. Feingold, and D. P. Arovas, Phys. Rev. Lett. **65**, 3076 (1990).
 - [9] R. Lima and D. Shepelyansky, Phys. Rev. Lett. **67**, 1377 (1991).
 - [10] T. Prosen, I. Satija, and N. Shah, Phys. Rev. Lett. **87**, 066601 (2001).
 - [11] R. Ketzmerick, K. Kruse, and T. Geisel, Physica D **131**, 247 (1999).
 - [12] S. Fishman, I. Guarneri, and L. Rebuzzini, Phys. Rev. Lett. **89**, 084101 (2002); M. K. Oberthaler, R. M. Godun, M. B. d'Arcy, G. S. Summy, and K. Burnett, *ibid.* **83**, 4447 (1999).
 - [13] F. Keck, H. J. Korsch, and S. Mossmann, J. Phys. A **36**, 2125 (2003).
 - [14] B. V. Chirikov, Phys. Rep. **52**, 263 (1979); A. Iomin and G. Zaslavsky, Phys. Rev. E **60**, 7580 (1999).
 - [15] R. Fleishmann, T. Geisel, R. Ketzmerick, and G. Petschel, Physica D **86**, 171 (1995); A. Iomin and S. Fishman, Phys. Rev. B **61**, 2085 (2000).